between 0.90 μm and 0.70 μm, but we are unable to determine this due to the limited wavelength sampling of the data. The long-wavelength extinction law determined by Elias, Frogel, and Humphreys (1985), which is based on data for stars with a variety of values of R_V, is completely consistent with the RL law. There are minor differences between the various near-IR extinction laws when presented in terms of color-excess ratios [e.g., $E(J-H)/E(H-K)$], but we have not investigated their origins. The increased scatter in $A(\lambda)/A(I)$ is another reason for presenting the results in terms of $A(\lambda)/A(V)$, even though the normalization to $A(V)$ produces a spurious dependence on R_V which is not really presented at wavelengths longer than about 0.9 μm.

The filled symbols in Figure 2 represent data for a subset of the FM sample for which data at R, I, and J were available. The open symbols represent a large sample of additional data for which we had optical/NIR photometry. Most of these data come from the list given in Clayton and Cardelli (1988). As with Figure 1*b*, these data, which number 70 lines of sight, clearly show that the behavior exhibited by the FM sample is a good representation of the average R_V-dependence. The "error" bars shown in the figure represent mean uncertainties calculated via a propagation-of-errors analysis using the adopted mean observational color errors discussed in CCM and calculated uncertainties in the derived $A(V)$ values. Although the scatter within the relationships shown in Figure 2 may represent real systematic deviations from the mean, the scatter is within the limits of the observational uncertainties.

b) *Parameterization: The Average R_V-dependent Extinction Law*

Using NIR and optical data for stars in FM sample, we have extended the fitting of $\langle A(\lambda)/A(V)\rangle$, the mean extinction law, to the range 0.3 μm^{-1}–3.3 μm^{-1}, while CCM considered only 3.2 $\mu m^{-1} < x < 8$ μm^{-1}. The procedure was the same as the one used by CCM and involved deriving the least-squares coefficients a_i and b_i from a linear fit to $A(\lambda_i)/A(V)$ versus R_V^{-1} at all the optical passband wavelengths (see Table 3). The wavelength-dependent coefficients $a(x)$ and $b(x)$ were then fitted with a polynomial in x, in units of μm^{-1}. The mean R_V-dependent extinction law then takes the form

$$\langle A(\lambda)/A(V)\rangle = a(x) + b(x)/R_V \ . \quad (1)$$

For computational reasons, the complete extinction curve (0.3 μm^{-1}–8 μm^{-1}) has been divided into three wavelengths regions: *infrared* ($\lambda \geq 0.9$ μm), *optical/NIR* (0.9 $\mu m \geq \lambda \geq 0.3$ μm), and *ultraviolet* (0.3 $\mu m \geq \lambda \geq 0.125$ μm). In addition, a *far-ultraviolet* (0.125 $\mu m \geq \lambda \geq 0.10$ μm) segment has been added. The far-UV segment is based on only limited data (York *et al.* 1973; Snow and York 1975; Jenkins, Savage, and Spitzer 1986) and is therefore more uncertain. The division of the complete curve into segments is also practical in that it roughly defines different instrument/observing regimes. The results are discussed below.

i) *The Infrared and Optical*

Infrared: 0.3 $\mu m^{-1} \leq x \leq 1.1$ μm^{-1};

$$a(x) = 0.574x^{1.61} \ ; \quad (2a)$$

$$b(x) = -0.527x^{1.61} \ . \quad (2b)$$

Optical/NIR: 1.1 $\mu m^{-1} \leq x \leq 3.3$ μm^{-1} and $y = (x - 1.82)$;

$$a(x) = 1 + 0.17699y - 0.50447y^2 - 0.02427y^3 + 0.72085y^4 + 0.01979y^5 - 0.77530y^6 + 0.32999y^7 \ ; \quad (3a)$$

$$b(x) = 1.41338y + 2.28305y^2 + 1.07233y^3 - 5.38434y^4 - 0.62251y^5 + 5.30260y^6 - 2.09002y^7 \ . \quad (3b)$$

Figure 3 shows a comparison of the computed optical/NIR portion of the curve from equations (2) and (3) with data for three lines of sight with widely separated values of R_V. The positions of the different passbands are also labeled. The fit is quite good for all three lines of sight. Because $A(\lambda)/A(I)$ seems independent of R_V for $\lambda \geq 0.9$ μm, the segment for $x \leq 1.1$ μm^{-1} was derived by fitting the data of RL with a power law.

TABLE 3

COEFFICIENTS AND EXTINCTION AT STANDARD OPTICAL/NEAR-IR WAVELENGTHS

				$A(\lambda)/A(V)$ for $R_V = 3.1$		
FILTER	x (μm^{-1})	$a(x)$[a]	$b(x)$[a]	$a(x) + b(x)/R_V$	SM79[b]	RL[c]
U	2.78	0.9530	1.9090	1.569	...	1.531
B	2.27	0.9982	1.0495	1.337	1.322	1.325
V	1.82	1.0000	0.0000	1.000	1.000	1.000
R	1.43	0.8686	−0.3660	0.751	0.748	0.748
I	1.11	0.6800	−0.6239	0.479	0.484	0.482
J	0.80	0.4008	−0.3679	0.282	0.281	0.282
H	0.63	0.2693	−0.2473	0.190	...	0.175
K	0.46	0.1615	−0.1483	0.114	0.123	0.112
L	0.29	0.0800	−0.0734	0.056	0.052	0.058

[a] Derived from eqs. (2) and (3).
[b] From Savage and Mathis (1979) for their adopted R_V of 3.1.
[c] From Rieke and Lebofsky (1985) for their adopted R_V value of 3.1.

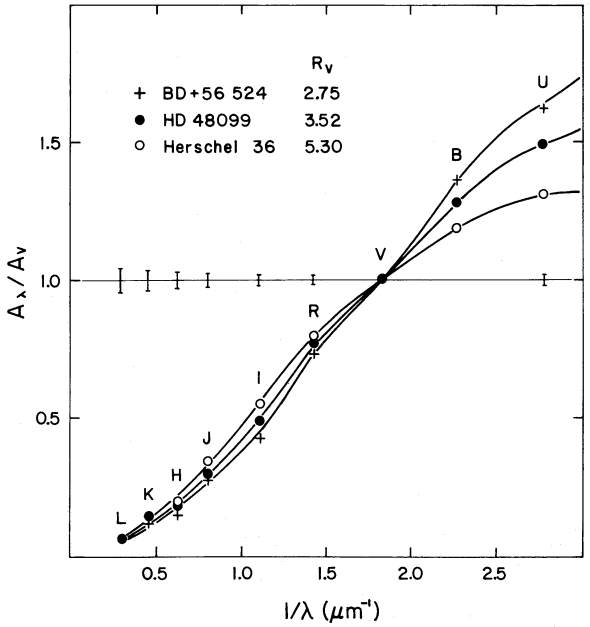

FIG. 3.—Comparison between the mean optical/NIR R_V-dependent extinction law from eqs. (2) and (3) and three lines of sight with largely separated R_V values. The wavelength position of the various broad-band filters from which the data were obtained are labeled (see Table 3). The "error" bars represent the computed standard deviation of the data about the best fit of $A(\lambda)/A(V)$ vs. R_V^{-1} with $a(x) + b(x)/R_V$ where $x \equiv \lambda^{-1}$. The effect of varying R_V on the shape of the extinction curves is quite apparent, particularly at the shorter wavelengths.

The equation for the segment 1.1 $\mu m^{-1} \leq x \leq 3.3$ μm^{-1} was found by fitting a seventh-order polynomial to $a(x)$ and $b(x)$ derived from $A(\lambda)/A(V)$ versus R_V^{-1} at the passbands I through U and the UV point at $x = 3.3$ μm^{-1}. The "error" bars shown in the figure are the standard deviations of the data at each passband about the best fit. Very likely, they do not represent true errors, but rather the real deviations of various lines of sight from the mean. Although we only have data at the wavelengths indicated, a polynomial was used in order to allow the mean extinction to be directly calculated at all wavelengths. (A preliminary optical/NIR extinction law was given in Cardelli, Clayton, and Mathis 1989. While that law reproduces the average R_V-dependent extinction reasonably well, we consider the results of eqs. [3a] and [3b] as a more accurate representation.)

How do our R_V-dependent results compare to standard average curves? Table 3 lists the values of $a(x)$, $b(x)$, and $A(\lambda)/A(V)$ for $R_V = 3.1$ from equations (2) and (3) at the various wavelengths where data were available, along with $A(\lambda)/A(V)$ for the same R_V from the average curves of Savage and Mathis (1979; SM79) and RL. The agreement is quite good at all wavelengths. Comparison between $A(\lambda)/A(V)$ from equations (2) and (3) and a spline or interpolation of the SM and RL data for other wavelengths indicates no significant deviation between B and L (this is only a comparison to using SM or RL, and does not include the presence of *real* structure). However, our polynomial shows a slight enhancement in extinction, or hump, between B and U amounting to $+0.05$ at $x = 2.50$ μm^{-1}. This hump is not present in the data of SM79 and is probably due to our fit. Consequently, the *R_V-dependent* results of equations (2) and (3) can be equally reproduced (without the hump) from a spline fit or interpolation of the values of $a(x)$ and $b(x)$ supplied in Table 2.

How does our function compare to higher resolution curves? The well-known Whitford (1958) extinction law, recently confirmed by Ardeberg and Virdefors (1982), has two segments, linear in x, joining at $x = 2.25$ μm^{-1} (see also Underhill and Walker 1966). Because the optical portion of our polynomial extinction law was derived from broad-band data, equation (2) does not have the abrupt change in slope (perhaps the hump produced from our polynomial fit is a consequence of this rapid change in slope). The Whitford law may therefore be more accurate for the diffuse ISM near $x \approx 2.25$ μm^{-1}. The virtue of ours, however, is that it joins smoothly onto the UV extinction law from the FM sample of stars, and that it takes into account the *differences in the extinction laws of lines of sight with various values of R_V*. Our extinction law also does not contain any of the very broad band structure which has been reported in the optical extinction law (Hayes *et al.* 1973; Schild 1977; Walker *et al.* 1980; Krelowski, Maszkowski, and Strobel 1986). We have not analyzed the data upon which the Whitford law was based to see if there are any effects introduced by combining lines of sight with different values of R_V into the same mean law.

ii) *The Ultraviolet and Far-UV*

Ultraviolet: 3.3 $\mu m^{-1} \leq x \leq 8$ μm^{-1};

$$a(x) = 1.752 - 0.316x - 0.104/[(x - 4.67)^2 + 0.341] + F_a(x) \quad (4a)$$

$$b(x) = -3.090 + 1.825x + 1.206/[(x - 4.62)^2 + 0.263] + F_b(x) \quad (4b)$$

$$F_a(x) = -0.04473(x - 5.9)^2 - 0.009779(x - 5.9)^3 \quad (8 \geq x \geq 5.9)$$

$$F_b(x) = 0.2130(x - 5.9)^2 + 0.1207(x - 5.9)^3 \quad (8 \geq x \geq 5.9)$$

$$F_a(x) = F_b(x) = 0 \quad (x < 5.9)$$

Figure 4 shows a comparison between our R_V-dependent extinction law from 0.3 $\mu m^{-1} \leq x \leq 8$ μm^{-1} for the same three lines of sight shown in Figure 3. Because the curves are closely spaced in the optical/NIR, only the optical data at U, B, and V have been shown. The agreement is quite good, especially for Her 36 and BD +56°524. HD 48099 has been shown, because it represents one of the poorer fits in the sample. Again, the "error" bars shown in the figure are the standard deviations of the data (e.g., Fig. 1*a*) about the best fit. (Eq. [4] is identical with the one found in CCM with the exception of the first term in eq. [4a], which has been decreased by 0.05. This decrease represents only a zero-point shift in the UV curve presented by CCM and was found to be necessary in order to smoothly join the optical with the UV. Such a small shift is well within the dispersion of the data.)

As with the optical/NIR, one test of the consistency of the above UV expressions is to compare reddening corrections produced using equation (4) with existing average curves, the most quoted of which are SM79 and Seaton (1979; S79). In the case of equation (4), the appropriate R_V value is adopted to be 3.1–3.2. Differences between normalized reddening corrections, $A(\lambda)/A(V)$, produced from equation (4) and those from the

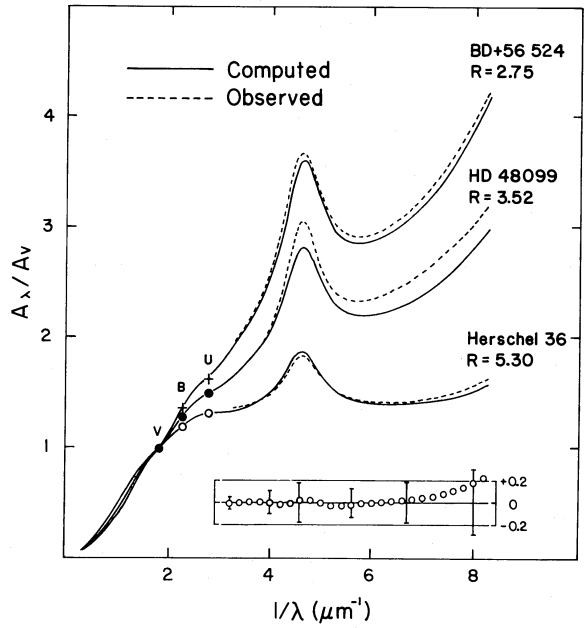

FIG. 4.—Same as Fig. 3 except for the UV portion of the mean R_V-dependent extinction law from eq. (4). The data at U, B, and V from Fig. 3 are also plotted. Again, the "error" bars in the lower inset represent the computed standard deviation of the data about the best fit of $A(\lambda)/A(V)$ vs. R_V^{-1} with $a(x) + b(x)/R_V$. The open symbols in the inset represent the difference between $A(\lambda)/A(V)$ from eq. (4) and the average curve of Seaton (1979) for $R_V = 3.2$. The only serious deviation occurs for $x > 7$ μm^{-1} (see text).